Near Real Time Confocal Microscopy of Amelanotic Tissue: Dynamics of Aceto-Whitening Enable Nuclear Segmentation

Tom Collier, Peggy Shen BS, Benoit de Pradier, MS, Kung-Bin Sung MS and Rebecca Richards-Kortum, PhD

Department of Electrical and Computer Engineering, The University of Texas at Austin, Austin, Texas 78712

collier@mail.utexas.edu

Anais Malpica, MD and Michele Follen, MD, MS

Departments of Pathology and Gynecologic Oncology, The University of Texas M.D. Anderson Cancer Center, Houston, Texas 78730

Abstract: High resolution, *in vivo* confocal imaging of amelanotic epithelial tissue may offer a clinically useful adjunct to standard histopathologic techniques. Application of acetic acid has been shown to enhance contrast in confocal images of these tissues.   In this study, we record the time course of aceto-whitening at the cellular level and determine whether the contrast provided enables quantitative feature analysis. Confocal images and videos of cervical specimens were obtained throughout the epithelium before, during and post-acetic acid after the application of 6% acetic acid.   Aceto-whitening occurs within seconds after the application. The confocal imaging system resolved sub-cellular detail throughout the entire epithelial thickness and provided sufficient contrast to enable quantitative feature analysis.

©2000 Optical Society of America

OCIS codes: (180.1790) Confocal Microscopy; (170.3880) Medical and Biological Imaging

---

References and Links

1. D.M. Parkin, P. Pisani, J. Ferlay Estimates of the Worldwide Incidence of Eighteen Major Cancers in 1985. Int. J. Cancer 1993; **54**,594-606
2. G. Dallen Bach-Hellueg, H. Doulson, *Histopathology of the Cervix Uteri*, (Springer-Verlag New York Inc., 1990)
3. V. Jester, P. M. Andrews, W. M. Petroll, M. A. Lemp, and H. D. Cavanaugh, *"In vivo,* real-time confocal imaging," L Electron Microsc. Tech. **18**, 50-60 (1991).
4. J. V. Jester, W. M. Petrull, R. M. Garana, M. A. Lemp, and H. D. Cavanaugh, "Comparison *of in vivo* and *ex vivo* cellular structure in rabbit eyes detected by tandem scanning microscopy," I. Microsc. **165**, 169-181 (1992).
5. B. Masters and A. A. Thaer, "Real-time scanning slit confocal microscopy of the *in vivo* human cornea," AppI. Opt. **33**, 695-701 (1994).
6. C. Bertrand and P. Corcuff, *"In vivo* spatio-temporal visualization of the human skin by real time confocal microscopy," Scanning **16**, 150-154 (1994).
7. P. Corcuff, G. Gonnord, G.E. Pierard, and J. L. Leveque, *"In vivo* microscopy of human skin: A new design for cosmetology and dermatology," Scanning **18,** 351-355 (1996).
8. Rajadhyaksha, M. Grossman, D. Esterowitz, R. H. Webb, and R. R. Anderson, *"In vivo* confocal scanning laser microscopy of human skin: Melanin provides strong contrast," I. Invest. Dermatol. **104**, 946952 (1995).
9. B. R. Masters, U. I. Aziz, A. F. Gmitro, J. H. Kerr, T. C. O'Grady, and L. Goldman, "Rapid observation of unfixed, unstained human skin biopsy specimens with confocal microscopy and visualization," L Biomed. Opt. **2**, 437~5 (1998).
10. C. L. Smithpeter, A. K. Dunn, A. I. Welch, and R. Richards-Kortum, "Penetration depth limits of *in vivo* confocal reflectance imaging," AppI. Opt. **37**, 2749-2754 (1998).
11. C. L. Smithpeter, A. Dunn, R. Drezek, T. Collier, R. Richards-Kortum, "Near Real Time Confocal

Microscopy of Cultured Amelanotic Cells: Sources of Signal, Contrast Agents and Limits of Contr*ast*," J ,
Biom. Opt., **3**,429-436, (1998)

12. R. Dresek, T. Collier, C. Brookner, R. Lotan, A. Malpica, R. Richards-Kortum, M. Follen, "Laser Scanning Confocal Microscopy of Cervical Tissue, Before and After Application of Acetic Acid," Am. J. of Obstetrics and Gynecology, paper under review.
13. L. Burke, D. Antonioli, B. Durcatman, *Colposcopy Text and Atlas*, (Appleton and Lange., 1991)
14. J. Thiran and B. Macq, "Morphological Feature Extraction for the Classification of Digital Images of Cancerous Tissues," IEEE Trans. Biomed., **43**, 1011-1020, (1996)
15. A. Gmitro and D. Aziz, "Confocal microscopy through a fiber-optic imaging bundle," Opt. Lett. **18**, 565-567 (1993).
16. R. Juskaitis, T. Wilson, and T.F. Watson, "Real time white light reflection confocal microscopy using a fiber-optic bundle," Scanning. **19**,15-19 (1997).
17. T. Dabbs and M. Glass, "Fiber-optic confocal microscope: FOCON," Appi. Opt **31**,3030-3035 (1992).
18. L. Giniunas, R. Juskaitis, and S.V. Shatalin, "Endoscope with optical sectioning capability," Appi. Opt. **32**, 2888-2890 (1993).
19. D.L. Dickensheets and G.S. Kino, "Micro-machined scanning confocal optical microscope," Opt. Lett. **21**, 764-766 (1996).

1. Introduction

Cancers of the epithelium of the cervix, urinary bladder, respiratory tract, oral mucosa, skin and colon are preceded by precancerous changes within the epithelium. Despite the presence of pre-cursor lesions, mortality for these cancers is significant[1]. Early detection represents the best opportunity to improve patient survival and quality of life; thus, new surveillance methods are needed to improve the ability to recognize pre-cancerous changes within epithelial tissues. Epithelial pre-cancers are associated with a variety of morphologic alterations, including increased nuclear size, increased nuclear/cytoplasmic ratio, hyperchromasia and pleomorphism[2].

Confocal imaging has been proposed as a new tool to non-invasively assess cell morphology using light reflected from tissue[3-9]. A pinhole placed at a conjugate image plane in the confocal microscope is used to localize reflected light in three dimensions with sufficient resolution to image individual cells and nuclei. Changes in refractive index provide contrast to recognize intracellular detail. In concept, this is similar to histological analysis of biopsy specimens, except three dimensional resolution is achieved without removing or physically sectioning tissue. Thus, confocal imaging provides a potential tool to detect pre-cancerous changes in the intact epithelium.

To date, much of the work using *in vivo* confocal imaging has focused on the eye[3-5] and skin[6-9] where melanin with its high refractive index (n=1.7) provides the primary source of contrast for imaging individual cells. Our group has shown[10-12] that confocal images of amelanotic cells have inherently less contrast. However, when epithelial cells[11] and tissue[12] are treated with weak acetic acid, the backscattering associated with the nucleus increases, providing additional contrast in confocal images. Acetic acid is commonly used to aid in the detection of cervical pre-cancer[13]. Precancerous areas of the cervix turn whitish 2-3 minutes after the application of 3-6% acetic acid, a phenomenon known as aceto-whitening.

The goals of this paper are to use confocal imaging to observe the time course of aceto-whitening at the cellular level and to determine whether the contrast provided enables quantitative feature analysis to quantitatively probe additional nuclear morphometry.

2. Experimental Methods

2.1 Confocal System

We designed and built an epi-illuminaiton confocal microscope (Figure 1). The light source is a continuous wave argon-ion pumped Ti:Sapphire laser tuned to 808 nm (890 Tunable Laser, Coherent). The beam is spatially filtered with a single mode optical fiber, collimated, and sent through a beam splitter to an x-y scanning system. The scanning mirrors are driven by a pair of galvanometers to produce a frame rate of 15 Hz (8000 kHz Video Scan Head,

General Scanning). The scanning lens, L1, focuses the beam at the back focal plane of a 25X 0.8 NA water immersion objective (Plan-Neofluar multi-immersion, Zeiss). 10-30 mW of power is focused to a 1 µm diameter spot on the sample. Light backscattered from the tissue returns to the beam splitter where it is reflected to the pinhole lens, L2, and focused through a 10 µm diameter pinhole. Light which passes through this pinhole is detected by an avalanche photodiode. The confocal system operates at a dimensionless pinhole radius of 2.5 to provide maximum optical sectioning for obtaining cellular detail. The scanning system is capable of scanning at variable angle ranges thus providing zoom capability. The measured lateral and axial resolution of the system are 0.8 um and 2-3 um respectively.
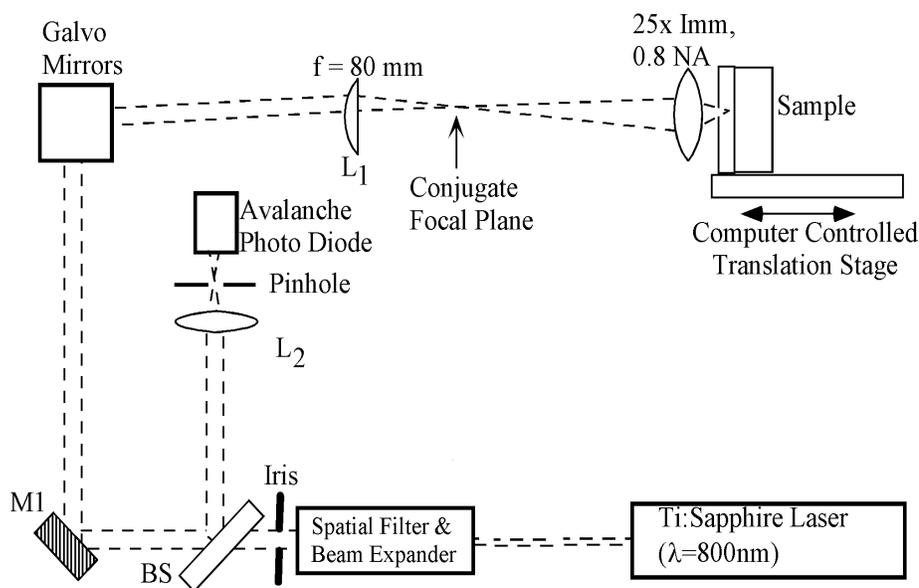

Figure 1. Set up of epi-illumination confocal microscope used to collect the images and video.

2.2 Specimens

Seven normal specimens of cervical tissue were obtained from seven patients following hysterectomy from the Southern Division of the Cooperative Human Tissue Network (CHTN) at The University of Alabama at Birmingham. The study was reviewed and approved by the Institutional Review Board at the University of Texas at Austin. One normal cervical biopsy was obtained from a patient undergoing colposcopy at the Colposcopy Clinic at the University of Texas M.D. Anderson Cancer Center. This patient was selected from a group of patients referred for follow-up colposcopy for suspected CIN on the basis of abnormal cervical cytology. Informed consent was obtained and the project was reviewed and approved by the Surveillance Committee at the University of Texas M.D. Anderson Cancer Center. The surgical samples were a minimum of 1 x 1 x 0.5 cm in size; the biopsy was 2-4 mm in size. All tissue specimens were frozen in liquid nitrogen immediately after collection and stored at -70°C until microscopic examination. Before imaging, each sample was thawed for 5-10 minutes in PBS.

2.3 Imaging

Video images were digitized using a video frame grabber card and displayed at 15 frames per second on a computer monitor. Individual bitmap images and avi video files were saved

from the frame grabber's video buffer. Confocal images were acquired from all eight samples before and after the application of acetic acid. Each biopsy was first imaged in PBS and image frames were acquired as the image plane was translated through various epithelial depths. A 6% solution of acetic acid was then added to each sample and image frames were acquired at various epithelial depths. Video was acquired from 2 of the 8 samples during and after addition of acetic acid. However, after addition of acetic acid, tissue swelling occurred which prevented the focus from remaining at a fixed depth. A 6% solution of acetic acid in isotonic PBS was applied to a third sample to prevent the swelling and video was acquired during and after this addition. After acetic acid was applied, video was acquired from four of the samples as the focus of the microscope was moved from the epithelial surface down to 200 um. In order to create a three-dimensional rendering of cell nuclei, images were obtained from two of the samples consecutively as the focus was moved at 1 um intervals through two cell layers after application of acetic acid. The 1 um interval was chosen to satisfy the Nyquist criteria for sampling with our system which has an axial resolution of 2-3 um. All samples were submitted for routine histologic analysis using hemotoxylin and eosin. Sections were examined by an experienced, board certified gynecologic pathologist (AM).

2.4 Image Processing

Each of the single frames presented here was resampled and processed to enhance the brightness and contrast. The brightness and contrast were increased by 22% and 53% respectively on each image taken before acetic acid, and 17% and 53% on each image taken after acetic acid. Brightness was enhanced by adding the noted percentage of full gray scale to each pixel; contrast was enhanced by removing the noted percentage of full gray scale from the image and expanding the remaining midrange gray levels. Resampling was performed to reduce the distortion in the images caused by nonlinearity in the resonant galvonometric scanning system. Linear interpolation was used to estimate pixel values. Each of the video files was compressed using Sorenson Video codec. No resampling was performed on the video images. The three dimensional rendering of the incremental image slices was performed using standard 3D surface rendering. Before rendering, the images were median filtered and thresholded to remove noise and smaller elements of the cells.

We developed a feature detection algorithm to detect and outline the cell nuclei, based on mathematical morphology, based on a modification of the approach of Thiran[14]. Briefly, this process consists of four steps. In the first, the image is thresholded to reduce noise and converted from grayscale to binary. Then the image is closed and then opened using flat, square structuring elements in order to remove all objects smaller than the nuclei. Next, the image is reconstructed using geodesic dilation to preserve the original shape of the nuclei. The reconstructed image is then closed again using a flat, square structuring element to reduce texture within the nucleus. Finally, the edges are identified to yield the nuclear contours. Twelve images from eight samples were processed with this algorithm. Eight of the images were of tissue treated with acetic acid; four were obtained pre-acetic acid. Brightness and contrast were not enhanced on any image before processing. The images were resampled as described above after processing.

3. Results

Figure 2 shows images of the tissue before acetic acid was applied. The cell outlines and nuclei can be clearly seen in most cells imaged near the epithelial surface (Fig 2a). As the focus is moved deeper, near the middle of the epithelium, the cell outlines can still be seen, but reflections from the nuclei are faint (Fig 2b). Most intra-cellular detail is lost in images taken near the bottom of the epithelium (data not shown). Figure 3 shows images taken after the application of acetic acid. Near the tissue surface the cell outlines are less visible, but the nuclei are dramatically brighter (Fig 3a). In the middle of the epithelium, the nuclei can still be clearly seen (Fig 3b). As the focus is moved near the bottom of the epithelium, 200 um

below the epithelial surface, the nuclei are faint but visible in the smaller cells near the basement membrane (Fig 3c). While these images were obtained from tissue which was previously frozen, confocal images of fresh cervical tissue show similar morphologic features, pre and post acetic acid [12].
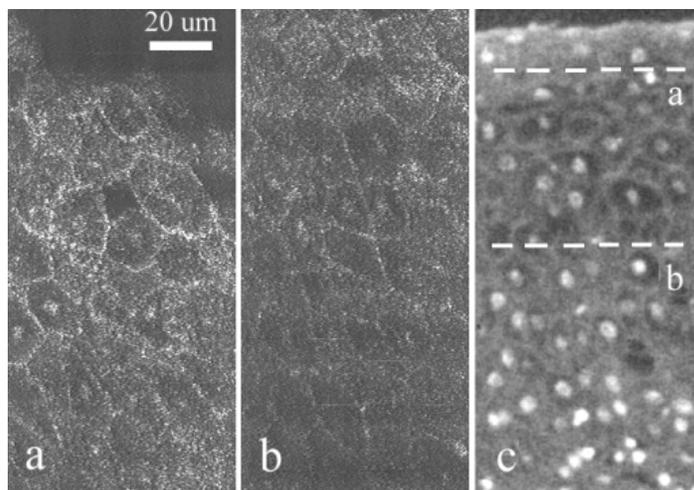

Figure 2. Images of cervical biopsy obtained prior to the application of acetic acid. a). Image taken with confocal microscope with the image plane parallel to the epithelial surface and the focus 20 microns below the surface. b). Same as (a), but with the focus 100 microns below the surface. c). Image of hemotoxylin and eosin stained transverse section using bright field microscopy. Contrast has been reversed in this black and white image to aid in comparing confocal and histologic images. Lines a and b indicate the approximate depth at which the confocal images in (a) and (b) were obtained.
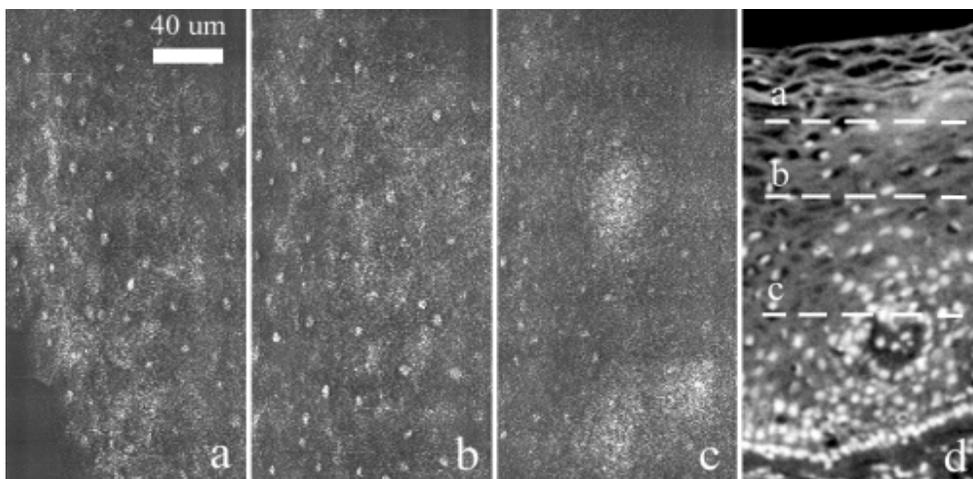

Figure 3. Images of cervical biopsy obtained after the application of acetic acid. a). Image taken with confocal microscope with the image plane parallel to the epithelial surface and the focus 50 microns below the surface. b). Same as (a) but with the focus 100 microns beneath the surface. c). Same as (a) but with the focus 200 microns beneath the surface. d). Image of hemotoxylin and eosin stained transverse section using bright field microscopy. Contrast has been reversed in this black and white image to aid in comparing confocal and histologic images. Lines a, b and c indicate the approximate depth at which the confocal images in (a), (b) and (c) were obtained.

The video in Figure 4 shows confocal images from a sample after the application of acetic acid as the image plane of the microscope is moved from the epithelial surface to the basement membrane, approximately 200 um deep; the field of view is 200 um. Nuclear size and density, important in the diagnosis of precancerous lesions, can be visualized in real time throughout the entire epithelium. As the image plane moved from the superficial epithelium to the basal epithelium, the size of the epithelial cells decreases as expected.

The video in Figure 5 illustrates the dynamic changes in nuclear backscattering as acetic acid is applied to the sample surface. Here, the image plane of the microscope was fixed 50 um beneath the epithelial surface, and the changes in image brightness and contrast are a result of the application of acetic acid; the field of view is 150 um. Nuclei, which are barely visible before the application of acetic acid, can clearly be seen afterwards, and the increase in nuclear backscattering is rapid following addition of acetic acid. Through image processing, nuclei can be isolated in three dimensions. Figure 6 shows a three dimensional rendering created from multiple images taken at higher zoom through a small field of nuclei; the field of view is 100 um.
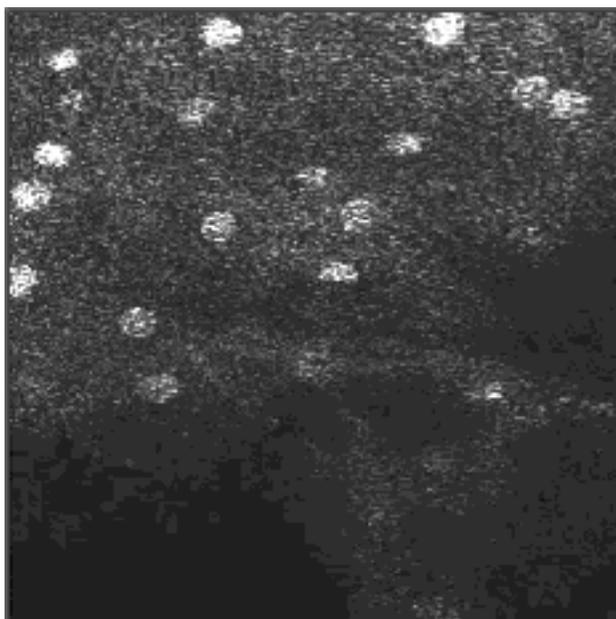

Figure 4. 3.1 MB Quicktime video of confocal images obtained as the image plane was translated from the epithelial surface to the basement membrane approximately 5 minutes after the application of acetic. The field of view is approximately 200 um.
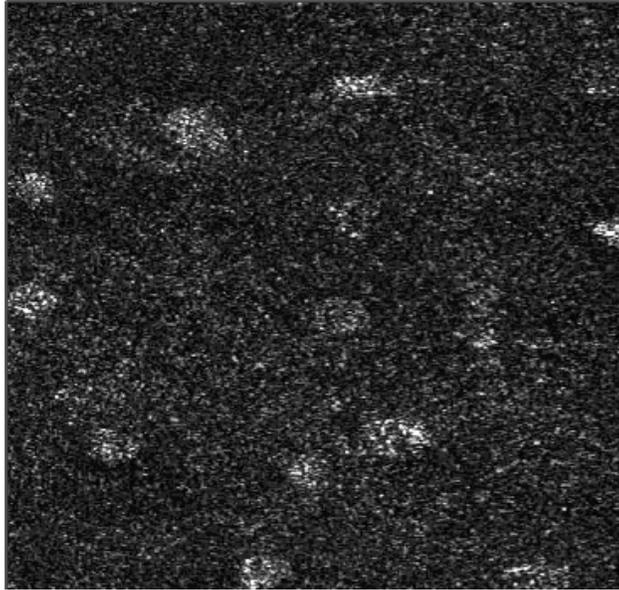
Figure 5. 3.1 MB Quicktime video of confocal images from a fixed image plane approximately 50 um below the epithelial surface as acetic acid is applied. The field of view is approximately 150 um.
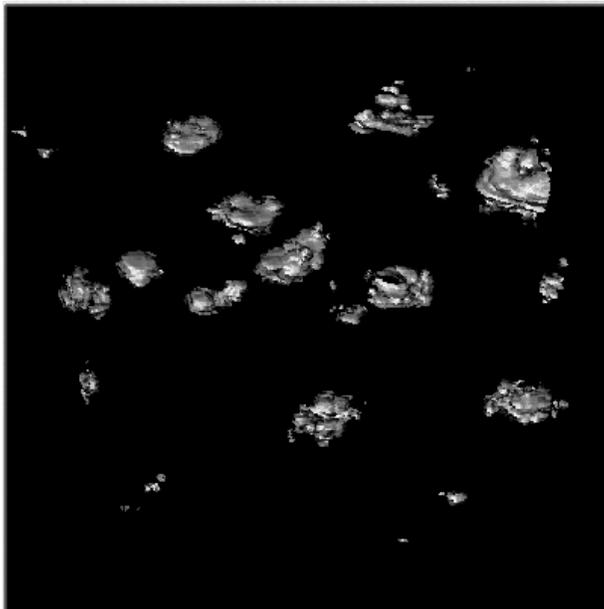

Figure 6. 2.4 MB Quicktime video of three dimensional rendering viewed from various angles. The rendering was created from 30 images taken at 1 um increments through 3 cell layers.

We applied the feature detection algorithm to images obtained before and after acetic acid to segment cell nuclei. For images acquired without acetic acid, features corresponding to nuclei, cell borders and noise were detected. (Fig 7). In images obtained after application of acetic acid, only nuclei were detected, and the nuclei were more accurately segmented. (Fig 8).
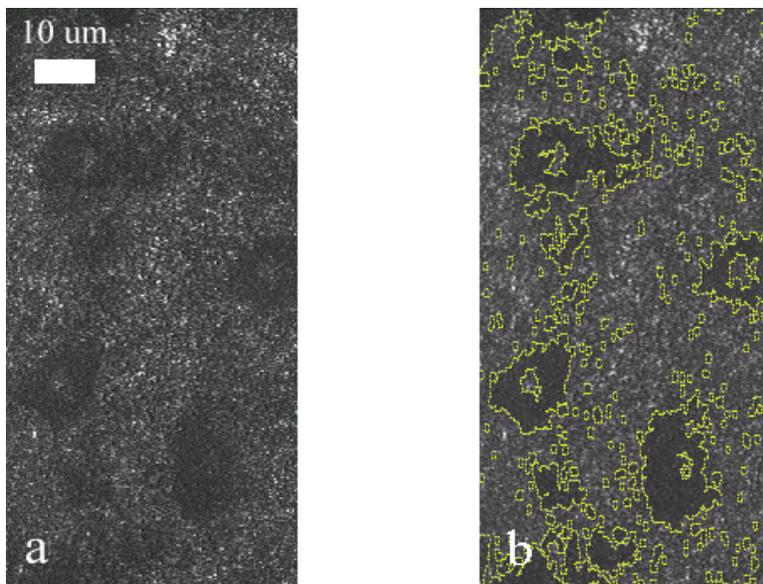

Figure 7. Segmentations of cell features with the feature detection algorithm on images taken without application of acetic acid. a). Unprocessed image of cervical biopsy. b). Same image as (a) with features outlined in yellow.
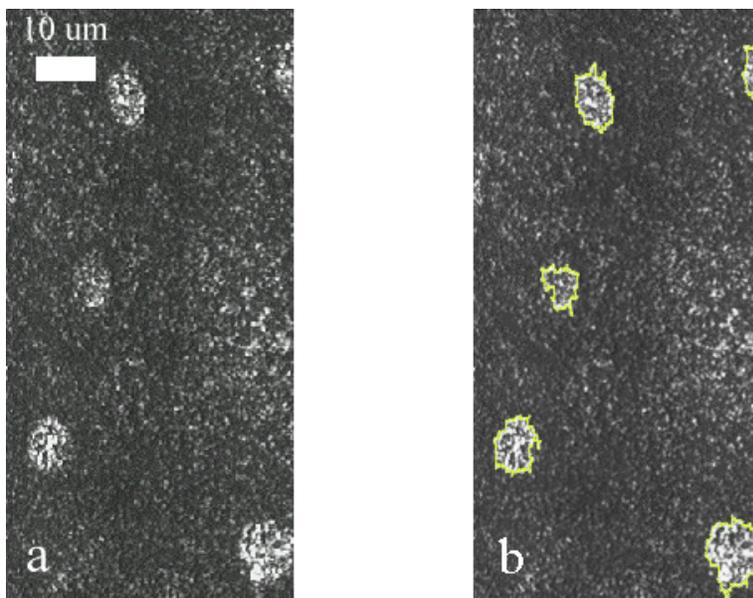

Figure 8. Segmentation of cell nuclei with our feature detection algorithm on images taken with the use of acetic acid. a). Unprocessed image of cervical biopsy. b). Same image as (a) with nuclei highlighted in yellow.

4. Discussion and Conclusions

Our results show that acetic acid rapidly increases the backscattering of cell nuclei in cervical tissue *in vitro* resulting in confocal images with increased contrast. Within seconds after the application of acetic acid, nuclei can be visualized throughout the entire epithelium. We have shown that the resulting image contrast is sufficient to enable nuclear segmentation and rendering in three dimensions. With further processing of the segmented images, it is possible to assess cell and tissue morphometry quantitatively, for example the nuclear/cytoplasmic ratio and nuclear deformity can be calculated[14]. These results suggest that confocal imaging following application of acetic acid may prove to be a useful tool in recognition of epithelial precancers since precancers are characterized by increased nuclear size, increased nuclear/cytoplasmic ratio, hyperchromasia and pleomorphism, which currently can only be assessed through biopsy. This method could be easily implemented clinically since acetic acid is already used in routine clinical examination of the cervix using colposcopy.

Many epithelial sites at risk for development of precancers are located in areas such as the bladder or lung which can be accessed with fiber optic endoscopes but not with conventional confocal microscopes. To access these sites, several fiber optic confocal microscopes have been developed[15-19], however all suffer from a lack of reflected light to provide sufficient contrast *in vivo*. The acetic acid technique described here shows the potential to increase the backscattered light necessary which may improve the S/N ratio of these fiber optic confocal endoscopes.

Acknowledgements